Supplement of

Measurement report: Effects of photochemical aging on the formation and evolution of summertime secondary aerosol in Beijing

Tianzeng Chen[a], Jun Liu[a, c], Qingxin Ma[a, b, c, *], Biwu Chu[a, b, c], Peng Zhang[a], Jinzhu Ma[a, b, c], Yongchun Liu[d], Cheng Zhong[a, c], Pengfei Liu[a], Yafei Wang[e], Yujing Mu[a, b, c], Hong He[a, b, c]

[a] State Key Joint Laboratory of Environment Simulation and Pollution Control, Research Center for Eco-Environmental Sciences, Chinese Academy of Sciences, Beijing 100085, China

[b] Center for Excellence in Regional Atmospheric Environment, Institute of Urban Environment, Chinese Academy of Sciences, Xiamen 361021, China

c University of Chinese Academy of Sciences, Beijing 100049, China

[d.] Beijing Advanced Innovation center for Soft Matter Science and Engineering, Beijing University of Chemical Technology, Beijing 100029, China

[e.]Beijing Institute of Petrochemical Technology, Beijing 102617, China

Corresponding author: qxma@rcees.ac.cn (Qingxin Ma)

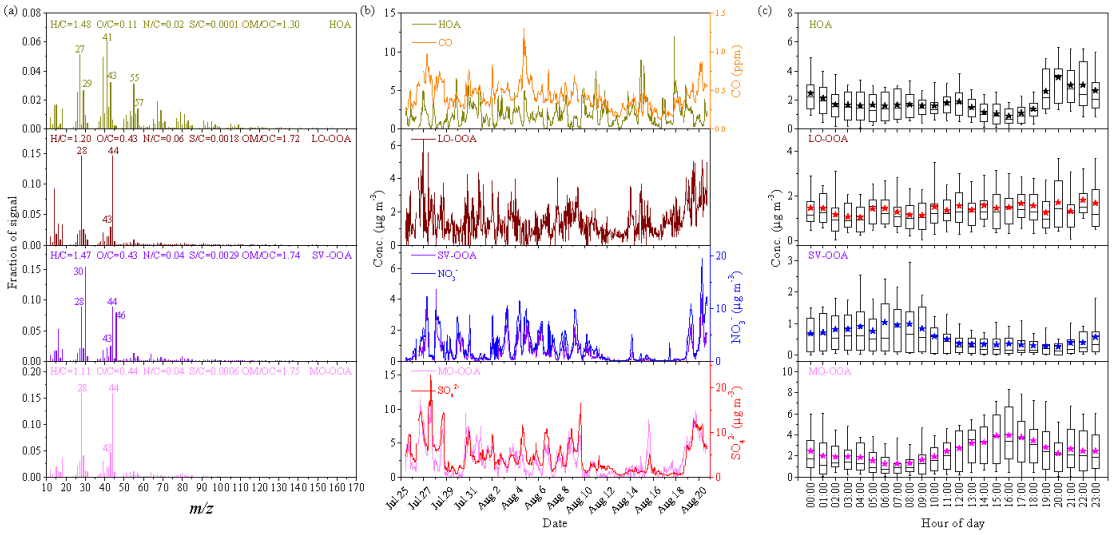

Figure S1. (a) Mass spectra, (b) time series, and (c) diurnal variation of the four factors (HOA, LO-OOA, SV-OOA and MO-OOA) identified from the PMF analysis to the HR-ToF-AMS data during the whole field observation. The upper and lower boundaries of boxes indicate the 75th and 25th percentiles; the line within the box marks the median; the whiskers above and below boxes indicate the 90th and 10th percentiles; and colored asterisk symbols represent the means.

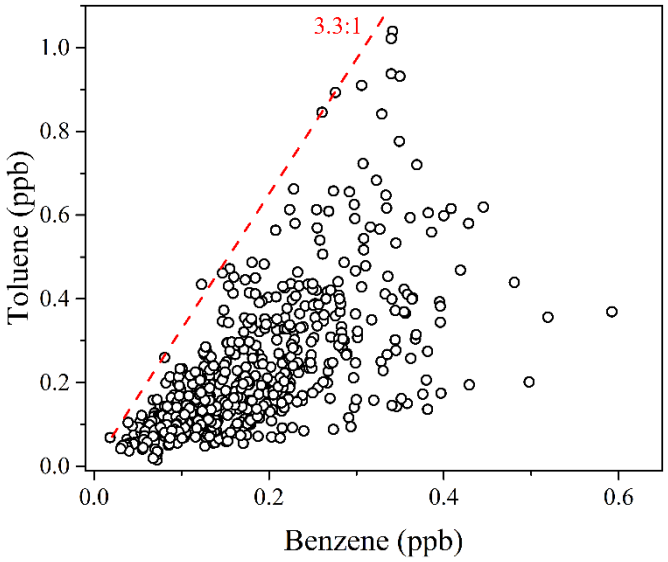

Figure S2. Scatter plot of toluene and benzene concentrations (black circle) during the whole field observation. The emission ratio of toluene to benzene is determined to be 3.3 shown as the red dot line in the figure.

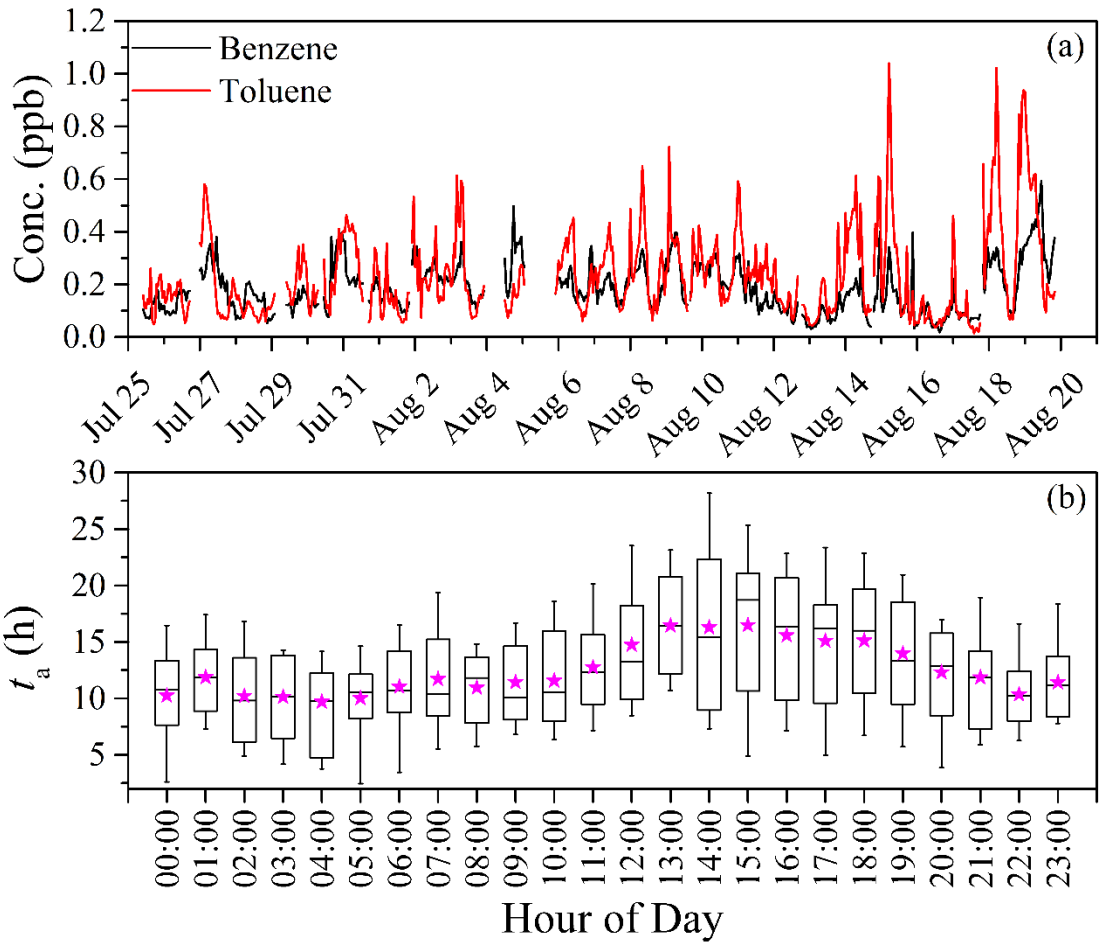

Figure S3. (a) Time series of concentrations of benzene and toluene, and (b) diurnal variation of calculated t_a during the whole field observation.

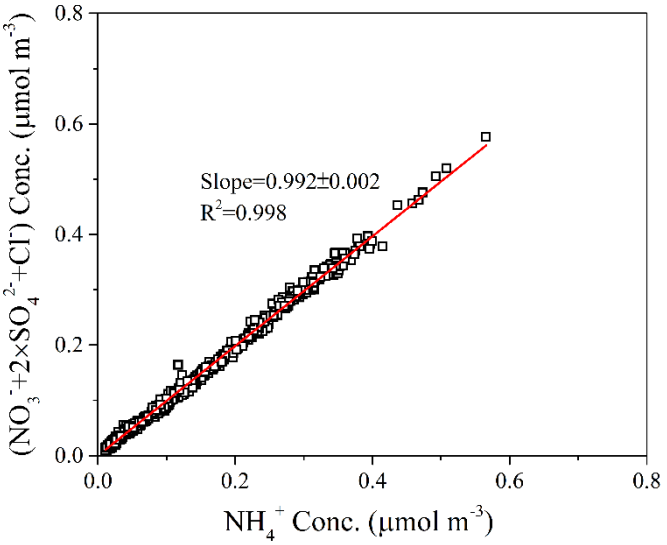

Figure S4. Linear relationship between $NO_3^-+2\times SO_4^{2-}+Cl^-$ and NH_4^+ measured by the HR-ToF-AMS.

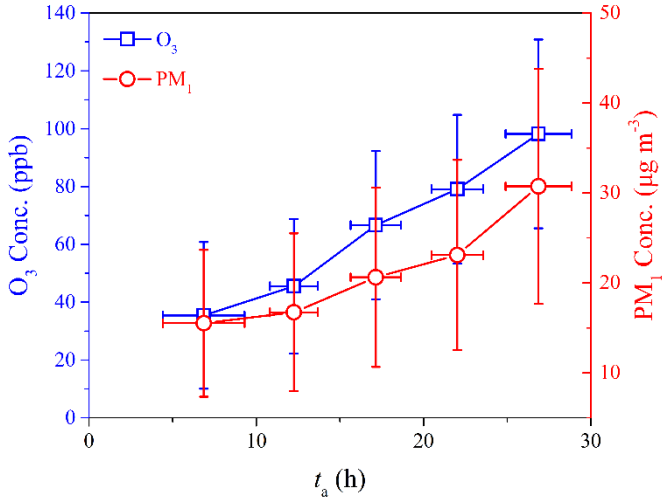

Figure S5. Variations of mass concentrations of O_3 and NR-PM_1 as a function of t_a. The data are binned according to the value of t_a (5 h increment).

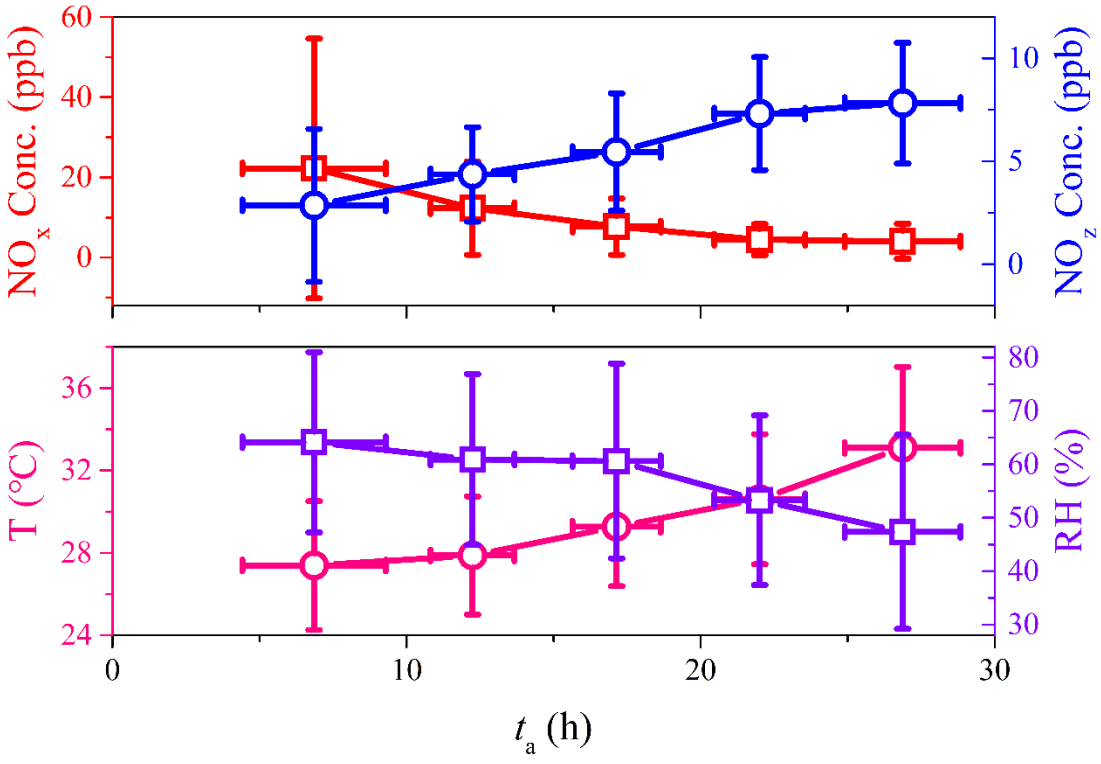

Figure S6. Variations of mass concentrations of NO_x, NO_z, and meteorological conditions (RH and T) as a function of t_a. The data are binned according to the value of t_a (5 h increment).

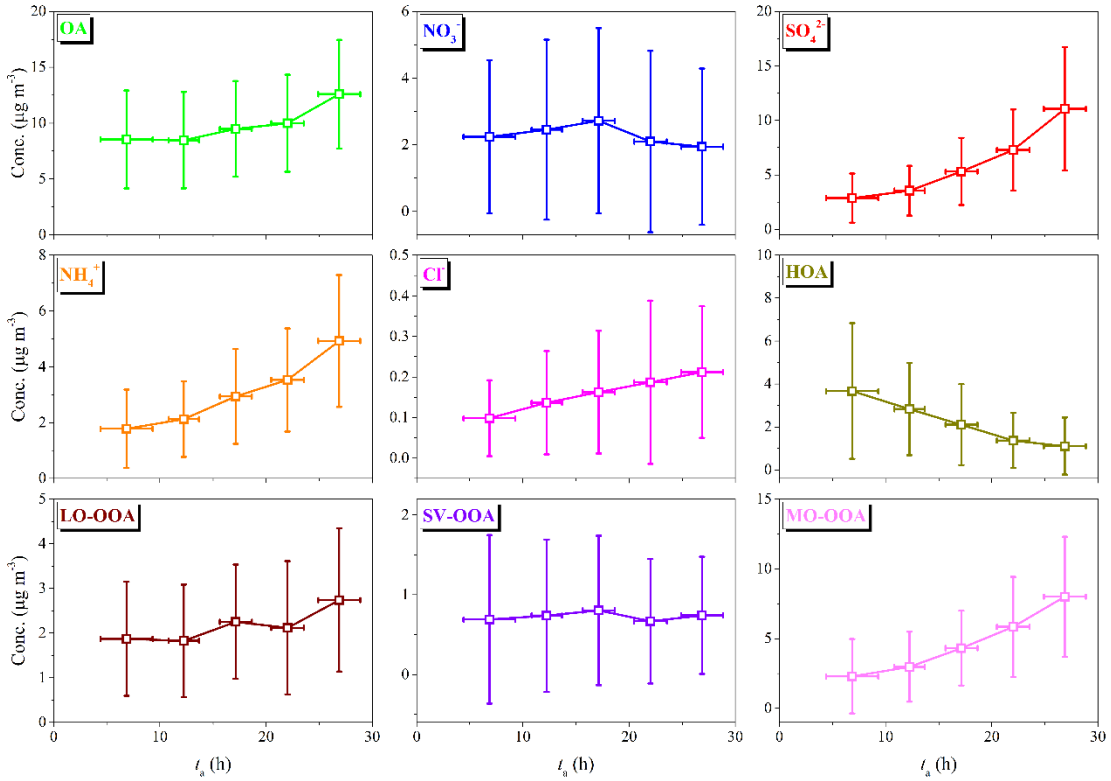

Figure S7. Variations of mass concentrations of NR-PM_1 species and OA factors as a function of t_a.

The data are binned according to the value of t_a (5 h increment).

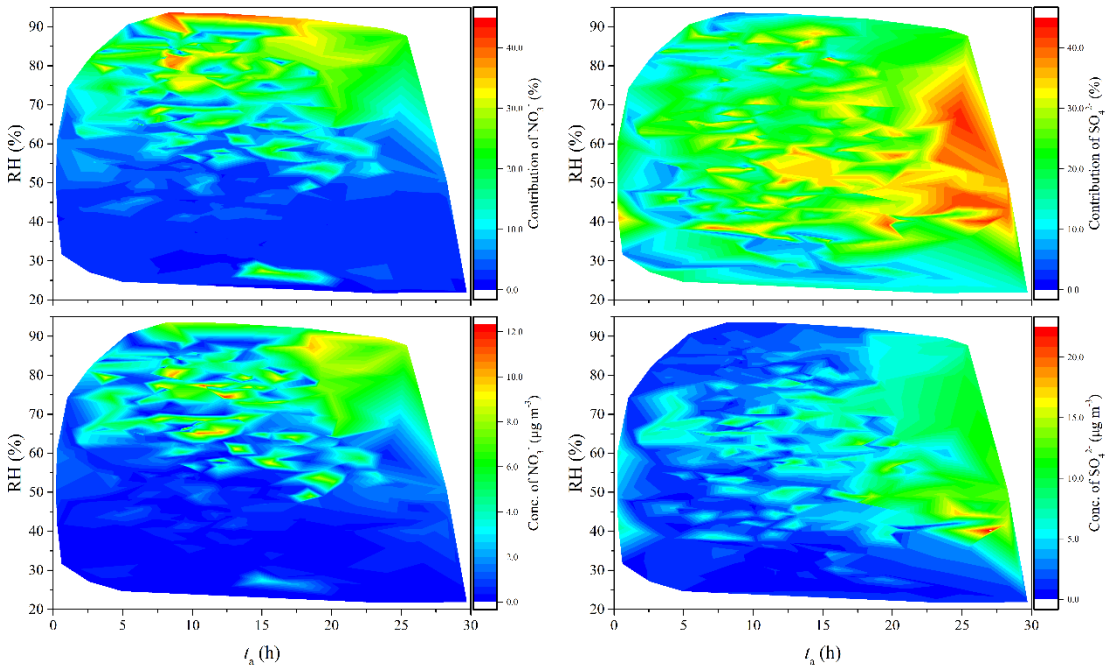

Figure S8. t_a- and RH-dependent distributions of NO_3^- and SO_4^{2-} during the whole field observation.

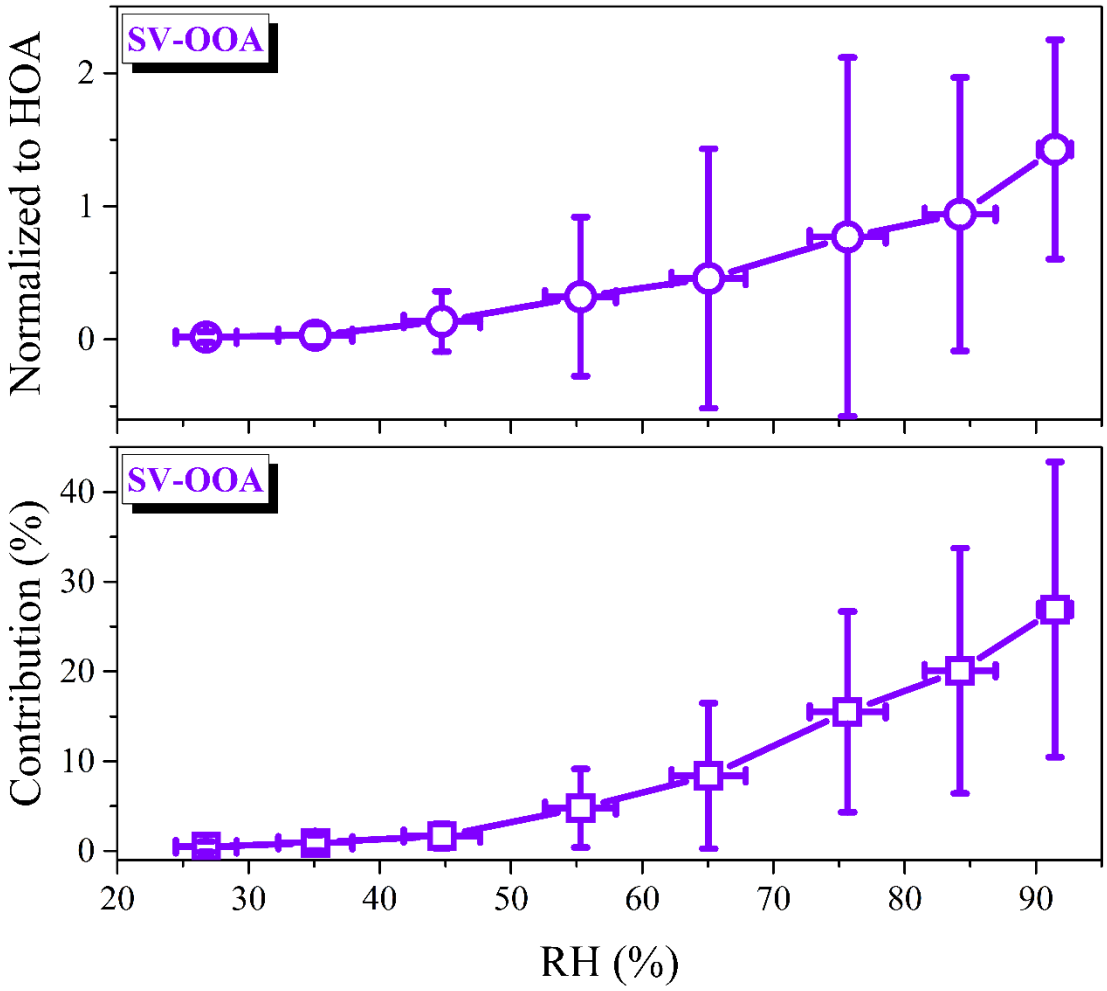

Figure S9. Variations of normalized mass concentration to HOA and contribution of SV-OOA as a function of RH. The data are binned according to RH (10 % increment).

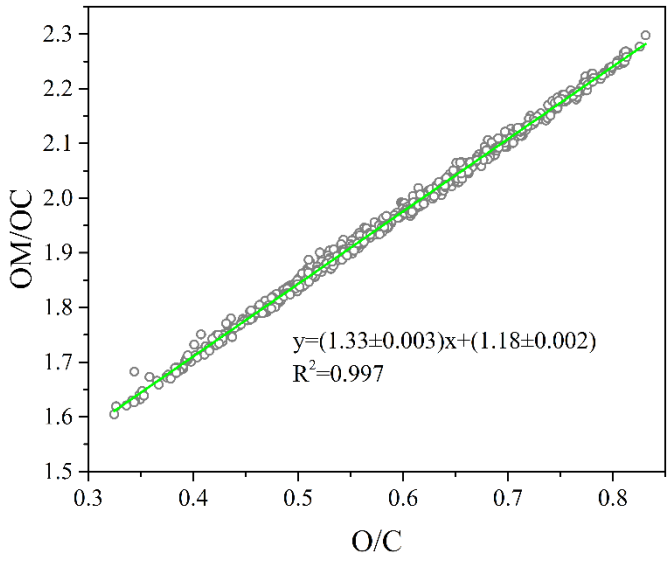

Figure S10. Relationship between OM/OC and O/C during this field observation.